*The Korean Journal of Ceramics*, **1** [1] 13-20 (1995)

# Effects of Thermal Annealing on Dielectric and Piezoelectric Properties of $Pb(Zn,Mg)_{1/3}Nb_{2/3}O_3$-$PbTiO_3$ System in the Vicinity of Morphotropic Phase Boundary

**Hyun M. Jang and Kyu-Mann Lee**

*Department of Materials Science and Engineering, Laboratory for Physical Chemistry of Dielectric Materials, Pohang University of Science and Technology (POSTECH), Pohang 790-784, Korea*

(Received February 8, 1995)

Effects of thermal annealing on the dielectric/piezoelectric properties of $Pb(Zn,Mg)_{1/3}Nb_{2/3}O_3$-$PbTiO_3$ ceramics (PZMN-PT with Zn/Mg = 6/4) were examined across the rhombohedral/tetragonal morphotropic phase boundary (MPB). Both the relative dielectric permittivity ($\varepsilon_r$) and the piezoelectric constant ($d_{33}$)/electromechanical coupling constant ($k_p$) were increased by thermal annealing (800°~900°C) after sintering at 1150°C for 1 hr. Based on the dielectric analysis using the series mixing model and the concept of a random distribution of the local Curie points, the observed improvements in the dielectric and piezoelectric properties of PZMN-PT were interpreted in terms of the elimination of PbO-rich amorphous intergranular layers (~1 nm) induced by thermal annealing. A concrete evidence of the presence of amorphous grain-boundary layers in the unannealed (as-sintered) specimen was obtained by examining the structure of intergranular region using a TEM.

***Key words*** : Lead zinc magnesium niobate ($Pb(Zn,Mg)_{1/3}Nb_{2/3}O_3$), Morphotropic phase boundary (MPB), Dielectric permittivity, Intergranular layer, Thermal annealing.

## I. Introduction

Lead zinc niobate, $Pb(Zn_{1/3}Nb_{2/3})O_3$ (PZN), is a relaxor type of ferroelectric material with a partially disordered perovskite structure. The solid solution of PZN, with rhombohedral symmetry, and $PbTiO_3$ (PT), with tetragonal symmetry, has a rhombohedral/tetragonal morphotropic phase boundary (MPB) near 10 mol % PT.[1] The single crystal of PZN-PT with a composition near the MPB exhibits the highest electromechanical coupling factor among all ferroelectrics,[2] together with excellent dielectric properties. It is very difficult, however, to prepare pure PZN-PT polycrystalline specimens with the perovskite structure by conventional ceramic processing. The reason behind the observed difficulties in the preparation of pure perovskite PZN or PZN-PT ceramics was examined using the single crystals prepared by the PbO flux method.[3,4] It has been found that the perovskite PZN or PZN-0.1PT is thermodynamically unstable over a wide range of temperature (600° to 1400°C), rapidly yielding pyrochlore phase and PbO as the decomposition products.[3] Therefore, thermodynamic instability rules out the possibility of synthesizing dense, polycrystalline perovskite ceramics without modifying the third thermodynamic variable, that is, pressure. This also explains why various advanced processing schemes including the columbite precursor route[5] and sol-gel processing[6] are not successful for the stabilization of perovskite phase in a pure, stoichiometric PZN composition.

To date, the most extensively studied ferroelectric relaxor material is $Pb(Mg_{1/3}Nb_{2/3})O_3$ (PMN). The large relative dielectric permittivity (at 1 kHz, $\varepsilon_r \cong 15000$ for ceramics and $\varepsilon_r > 20000$ for single crystals) and the broad ferroelectric transition temperature of PMN near room temperature make it one of the most attractive materials for advanced multilayer ceramic capacitors[7] and electrostrictive actuators.[8-10] Although it is also difficult to prepare pure perovskite PMN by conventional ceramic processing, the problem associated with pyrochlore formation can be effectively eliminated by employing the columbite precursor method.[5] Thus, the perovskite phase in the PMN system is either thermodynamically stable or strongly metastable (within a certain range of temperature), and the difficulties in the preparation of perovskite PMN are associated mainly with the kinetic factors caused by an inhomogeneous mixing of reactant oxides on the submicrometer scale.

In view of the facts discussed above, one would expect that the addition of PMN to PZN-PT above a certain critical concentration could possibly eliminate the problem of pyrochlore phase formation by stabilizing the perovskite phase, without appreciable loss of dielectric properties of the perovskite PZN-PT. This was recently demonstrated using a PZN-PMN-PT pseudoternary system [0.9(0.6PZN-0.4PMN)-0.1PT][11] prepared by the columbite

precursor route. Furthermore, since PZN-PMN-PT (or simply referred to as PZMN-PT) system is expected to form a morphotropic phase boundary, it is possible, in principle, to prepare PZMN-PT ceramics having excellent dielectric/piezoelectric properties for a composition above 10 mol% PT, i.e., (1-x){(1-y)PZN-yPMN}-xPT with $x > 0.1$ for $y > 0$.

In the present study, the PZMN-PT polycrystalline ceramics with Zn/Mg = 6/4 were prepared by the columbite precursor route, and the dielectric and piezoelectric properties were examined across the rhombohedral/tetragonal MPB. To further improve piezoelectric properties the PZMN-PT specimens were thermally annealed after sintering at 1150°C. Both the relative dielectric permittivity and the piezoelectric constant/electromechanical coupling constant were increased by the annealing (800~900°C). Based on the dielectric analysis and the microscopic examination, the observed improvements in the dielectric and piezoelectric properties were interpreted in terms of the elimination of PbO-rich amorphous intergranular layers (~1 nm) induced by thermal annealing.

## II. Experimental Procedure

Examination of the content of perovskite phase after sintering indicated that the minimum fraction of PMN needed for an effective stabilization of perovskite phase in the PZMN [ (1-y)PZN-yPMN ] system was 0.4.[11] Since we are interested in the stabilization of perovskite phase with a minimal amount of PMN, the PZMN-PT systems with Zn/Mg = 0.6/0.4 were used in the present study. A preliminary study indicated that rhombohedral phase in the PZMN-PT completely disappeared for PT > 32 mol%. Thus, the composition range of PZMN-PT ceramics chosen in the present study can be represented by (1-x){0.6PZN-0.4PMN}-xPT with $0 \leq x \leq 0.32$. Unless specified elsewhere, the composition (1-x){0.6PZN-0.4PMN}-xPT is abbreviated as (1-x)PZMN-xPT or simply PZMN-xPT hereafter.

The columbite precursor method[5] was used in the fabrication of PZMN-xPT ceramics. A detailed description of the preparation of PZMN-xPT powders using the columbite precursor route was given in a previous article.[11] PbO and $TiO_2$ were added to a stoichiometric mixture of two different types of columbite precursors, i.e., $MgNb_2O_6$ (MN) and $ZnNb_2O_6$ (ZN). The mixture was ball-milled, dried, and then calcined at 800°C for 4 hr.

After calcination, an additional ball-milling step was added to ensure a fine particle size before sintering. The dried powders were first pressed as disks and then cold-isostatically pressed under 190 MPa pressure. The pressed pellets were sintered at 1150°C for 1 hr with a cooling rate of 5°C/min. To limit PbO loss from the pellets, a PbO-rich atmosphere was maintained by placing $PbZrO_3$ powder inside the covered alumina crucible. For the examination of thermal annealing effects, the sintered pellets were first air-quenched to room temperature, instead of furnace cooling. The quenched specimens were then annealed either at 800°C or at 900°C for 4 hr, followed by air quenching to room temperature.

The bulk densities of sintered specimens were determined by the modified Archimedes' displacement method (ASTM C-20, the boiling water method). The relative amounts of pyrochlore and perovskite phases were determined using XRD patterns of heat-treated samples by measuring the major x-ray peak intensities for perovskite and pyrochlore phases, that is, (110) and (222), respectively. The percentage of perovskite phase was estimated using the following equation[9]:

$$\% \text{ perovskite} = \frac{I_{perov(110)}}{I_{perov(110)} + I_{pyro(222)}} \times 100 \quad (1)$$

The multiple peak separation method was used to estimate the relative fraction of coexisting phases for various contents of PT. For this purpose, the XRD peak at $2\theta \cong 45°$ was separated into two tetragonal peaks [(200) and (002)] and one rhombohedral peak [(200)] using the Gauss-Cauchy function. The relative phase fraction was then calculated by the following equation[12]:

$$\text{phase}(\%) = \frac{\text{integrated intensity of R (200) or T}\{(200) \text{ and } (002)\}}{\text{total integrated intensity at } 2\theta \cong 45°} \quad (2)$$

where T and R denote the coexisting tetragonal and rhombohedral phases, respectively.

The lattice constants (a,c) and rhombohedral angle ($\alpha$) were also calculated from XRD data using the following equations :

(tetragonal)

$$\frac{1}{d^2} = \frac{h^2 + k^2}{a^2} + \frac{l^2}{c^2}$$

(rhombohedral)

$$\frac{1}{d^2} = \frac{(h^2 + k^2 + l^2)\sin^2\alpha + 2(hk + kl + hl)(\cos^2\alpha - \cos\alpha)}{a^2(1 - 3\cos^2\alpha + 2\cos^3\alpha)} \quad (3)$$

Samples for dielectric measurements were prepared from sintered pellets by polishing the faces with SiC grinding paper (#1000) and then 1-μm diamond paste and electroding with silver paint. The silver-coated specimens were heat-treated at 590°C for 15 min. Dielectric measurements were carried out on an automated system, whereby a LCR meter (HP 4284) and a temperature-control box (Delta design 9023) were controlled by a desktop computer system. Temperature was measured using a Keithley 740 thermometer via a K-type thermocouple mounted directly on the ground electrode of the sample fixture. The dielectric measurements were carried out as the samples were cooled at a rate of 1°C/min, and the temperature range covered was 300° to 20°C.

Samples for piezoelectric measurements were silver-coated and were poled in a silicone oil bath at 60°C with

an applied field of 30 kV/cm for 5 min. The piezoelectric constant, $d_{33}$, was determined using a piezo d-meter (model CADT, Channel Products, Inc.). The electromechanical coupling constant ($k_p$, piezoelectric planar coupling coefficient) was calculated using the resonance and antiresonance frequencies determined with an impedance/gain phase analyzer (HP 4194A).

Samples for transmission electron microscopy (TEM) were mechanically polished to 100μm and dimpled from both sides to obtain a thickness of about 15μm at the center. Suitable TEM specimens were obtained by ion beam thinning using argon ions at 4 kV and incident angle of 15° to the specimen. Microscopic examination was carried out using a transmission electron microscope (Philips-CM 30) operated at 300 kV.

## III. Results and Discussion

### *1. Morphotropic phase boundary*

Analysis of the relative phase fraction in (1-x)PZMN-xPT system at room temperature indicates that rhombohedral and tetragonal phases coexist in the composition range for $0.2 \leq x \leq 0.3$ (i.e., between 20 and 30 mol% PT; Fig. 1). As shown in Fig. 1, the composition of the MPB is 24 mol% PT, that is, (1-x)PZMN-xPT or equivalently (1-x){0.6PZN-0.4PMN}-xPT with $x = 0.24$. Since the MPB of (1-x)PZN-xPT is represented by $x = 0.1$ at room temperature,[1] the result of Fig. 1 indicates that the MPB moves towards a PT-rich region as PMN is added to a PZN-PT pseudobinary system.

The rhombohedral angle decreases slightly as the composition moves towards the tetragonal-rich field and becomes 89.85° at the MPB composition (24 mol% PT). The axial ratio of the lattice parameters (c/a) is 1 at the MPB and increases gradually as the content of PT increases (Fig. 2).

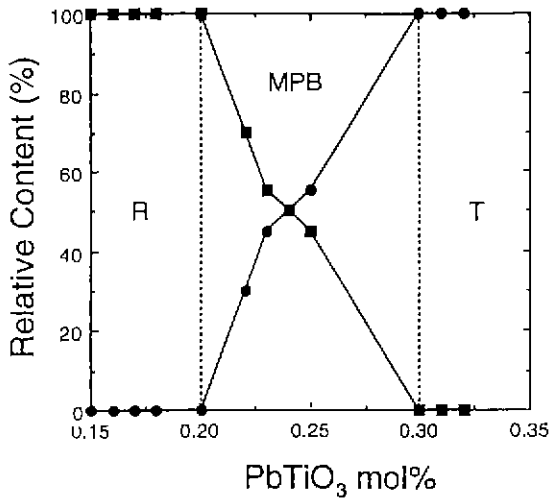


**Fig. 1.** Relative fraction of coexisting tetragonal and rhombohedral phases in PZMN-xPT system as a function of mole fraction of $PbTiO_3$ at room temperature.

### *2. Dielectric properties*

The relative dielectric permittivity versus temperature curves of (1-x) PZMN-xPT specimens containing various amounts of PT across the MPB (20~30 mol % PT) are shown in Fig. 3 for 1 kHz ac frequency. The temperature for the peak dielectric permittivity ($T_{max}$) increases systematically as the content of PT increases. Further examination of the data shown in Fig. 3 indicates that $T_{max}$ of PZMN-xPT system can be described by the application of the mixing rule to the three constituent oxides, that is, PMN ($T_{max}$ = -15°C),[13] PZN ($T_{max}$ = 140°C),[14,15] and PT ($T_{max}$ = 490°C).[16] In addition to these, the broadness of dielectric response increases as the content of PT decreases. The observed increase in the broadness of dielectric response with decreasing PT content reflects a gradual increase in relaxor characteristics (i.e., diffuse phase

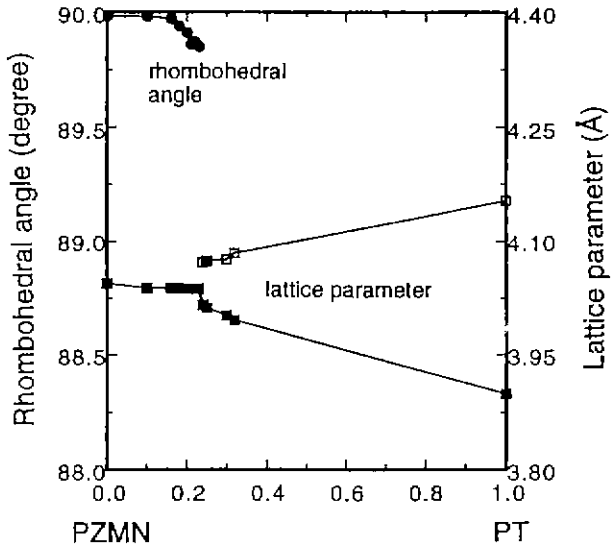


**Fig. 2.** Lattice parameters and rhombohedral angle of PZMN-xPT system at room temperature.

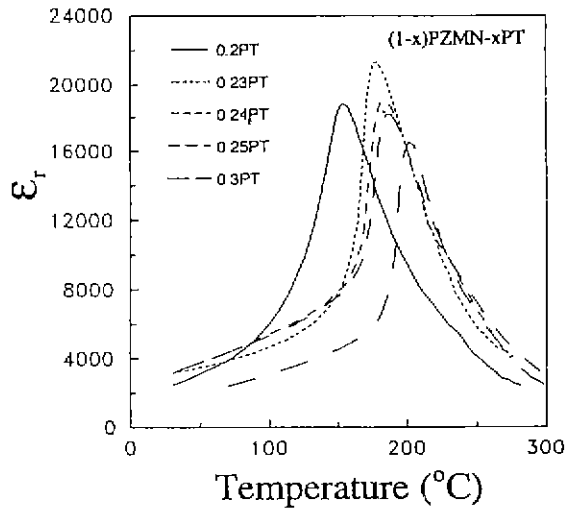


**Fig. 3.** Temperature-dependent relative dielectric permittivity of PZMN-xPT (at 1 kHz) containing various amounts of $PbTiO_3$.

transition and dielectric dispersion) as the system moves into the rhombohedral-rich side of the MPB.

As expected,[16] the maximum value of dielectric permittivity occurs near the MPB. However, the peak dielectric permittivity for 23 mol% PT is appreciably higher than that for the MPB composition (24 mol% PT). This observation can be explained in terms of the number of polarization directions in the MPB region.[17] In the tetragonal phase spontaneous polarization can occur along any of the three previously cubic [100] axes. However, there are 8 equivalent <111> directions in the rhombohedral crystal lattice with a 3m space group.[17] Therefore, PZMN-xPT at slightly rhombohedral-rich side of the MPB exhibits a larger net polarization than that exactly at the MPB.

To further improve dielectric/piezoelectric properties PZMN-xPT for the composition at the MPB (x=0.24) was annealed after sintering at 1150°C. The effect of thermal annealing on the dielectric properties of PZMN-0.24PT is illustrated in Fig. 4. The peak relative dielectric permittivity of PZMN-0.24PT increases from 18000 for the specimen sintered at 1150°C for 1 hr to 20500 for the specimen annealed at 800°C for 4 hr after the sintering.

The effect of annealing on the extent of diffuse phase transition (DPT) of PZMN-xPT was conveniently assessed by the Gaussian diffuseness plot. For relaxor ferroelectrics, Smolenskii[18] and Rolov[19] introduced the concept of a Gaussian distribution of the local Curie temperatures from which the diffuseness parameter (δ) for T > $T_{max}$ (or $T_o$) could be calculated. This can be formally written as

$$\frac{\varepsilon_g}{\varepsilon_m} = \exp\left[\frac{-(T-T_o)^2}{2\delta^2}\right] \quad (4)$$

where $\varepsilon_m$ is the maximum value of ($\varepsilon_{r,max}$), $\varepsilon_g$ is the inherent dielectric permittivity of perovskite grain at temperature T, and $T_o$ is the temperature at which $\varepsilon_m$ occurs. As clarified by Pilgrim et al.,[20] the estimate of δ using the above equation is valid for the temperature range where $\varepsilon_m/\varepsilon_g < 1.5$. As shown in Fig. 4(b), the extent of DPT (δ) is little affected or slightly increased by the annealing. In this plot, $\varepsilon_g$ was approximated by the measured dielectric permittivity ($\varepsilon_s$) of the PZMN-xPT specimen with x=0.24.

It has been known that the diffuse phase transition (DPT) in $Pb(B'_{1/3}B''_{2/3})O_3$-type perovskites is caused by the formation of 1:1 short-range ordered microdomains.[21,22] Since the average B′/B″ ratio in $Pb(B'_{1/3}B''_{2/3})O_3$-type perovskites is 1:2 (as opposed to 1:1 for the ordered microdomains), the enhanced 1:1 short-range ordering then increases the B-site compositional fluctuation occurring on a nanometer scale. It is now established that this microcompositional inhomogeneity is responsible for the DPT behavior in $Pb(B'_{1/3}B''_{2/3})O_3$-type perovskites.[11,21,22] Therefore, the result of Fig. 4 suggests that the extent of 1:1 short-range ordering or the B-site compositional fluctuation is essentially not influenced by the annealing. On the other hand, the thermal annealing increases the relative dielectric permittivity significantly [Fig. 4(a)].

There are several possible causes for the observed increase in the relative dielectric permittivity upon annealing. These could be (i) the change in the content and the location of pyrochlore phase, (ii) the increase in the density of sintered specimen, (iii) the increase in grain size, and (iv) the elimination of thin intergranular layers. Examination of the content of pyrochlore phase after the annealing at 800°C for 4 hr indicated that it was less than 2%, and the relative fraction of perovskite phase (> 0.98) was not affected by the post-thermal treatment at 800°C. Furthermore, the low-permittivity pyrochlore phase exists as discrete particles rather than intergranular layers.[23] Therefore, the presence of a small amount (< 2%) of pyrochlore phase is not related with the observed increase in the relative permittivity of PZMN-0.24PT annealed at 800°C for 4 hr. However, the content of pyrochlore phase slightly increased to 3% after the annealing at 900°C for 4 hr.

The microstructure of PZMN-0.24PT is unaffected by the annealing. The average grain size of PZMN-0.24PT is ~3 μm and, as expected, it is essentially independent

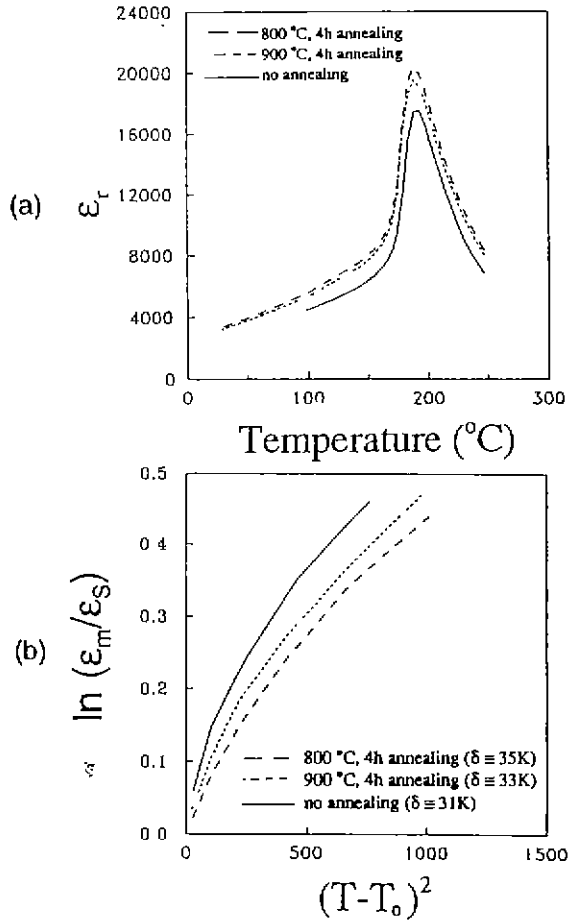


**Fig. 4.** Effects of thermal annealing on (a) relative dielectric permittivity and (b) quadratic temperature dependence of logarithmic dielectric permittivity of PZMN-0.24PT specimen at 1 kHz.

of thermal annealing (Fig. 5). The density of sintered PZMN-0.24PT specimen is 7.97 g/cm$^3$, regardless of the annealing in the temperature range between 800° and 900°C. Therefore, the elimination of low-permittivity intergranular layers by the thermal annealing seems to be mainly responsible for the observed increase in the relative dielectric permittivity.

### *3. Amorphous intergranular layer*

For PMN-based systems with excess PbO, the possibility of the existence of a low-permittivity intergranular phase was suggested and examined using the series mixing model.[11,23] It was concluded that the presence of the PbO-rich intergranular layer decreased the relative dielectric permittivity of PMN-based systems in the presence of excess PbO. Randall and co-workers[24] examined the structure of the PbO-rich intergranular layer and its effects on the dielectric properties of 0.93PMN-0.07PT system. Using TEM analysis, they showed that the thickness of the intergranular glassy phase was approximately 2 nm (20 Å). All these results suggest that the elimination of low-permittivity intergranular layers is directly related to the observed increase in the relative dielectric permittivity upon annealing (Fig. 4).

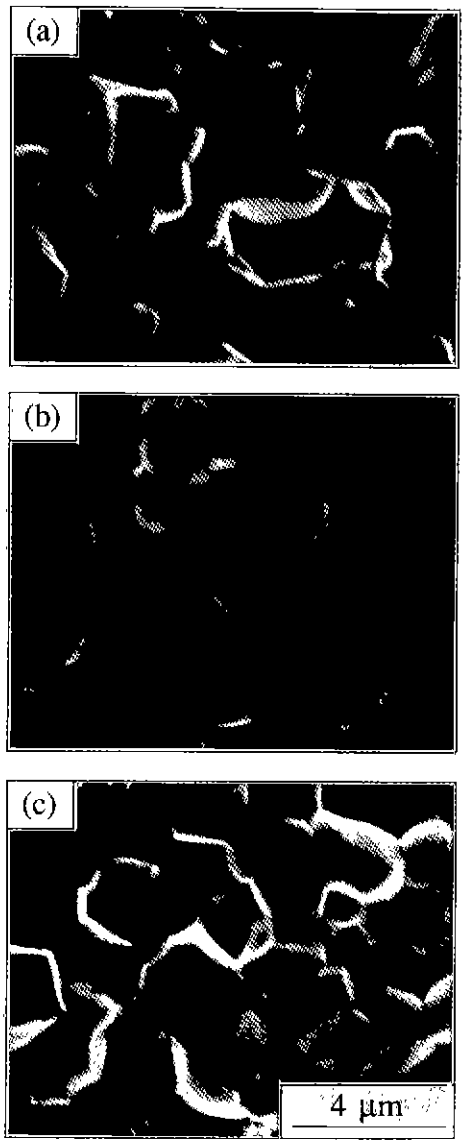


**Fig. 5.** Scanning electron micrographs of fractured surfaces of PZMN-0.24PT specimens sintered at 1150°C for 1 hr : (a) without thermal annealing, (b) annealed at 900°C for 4 hr, (c) annealed at 800°C for 4 hr.

According to the series mixing model for diphasic systems,[23] the relative dielectric permittivity of polycrystalline ceramics can be written as

$$\frac{D}{\varepsilon_c} = \frac{D_g}{\varepsilon_g} + \frac{D_{gb}}{\varepsilon_{gb}} \tag{5}$$

where $\varepsilon_c$ is the relative dielectric permittivity of specimen, $\varepsilon_g$ is the inherent dielectric permittivity of perovskite grain excluding the grain-boundary region, $\varepsilon_{gb}$ is that of the grain-boundary phase, $D_g$ is the thickness of the grain core, $D_{gb}$ is that of the grain-boundary region, and D is the total thickness of the grain (= $D_g$ + $D_{gb}$). $\varepsilon_{gb}$ is essentially independent of temperature. On the other hand, $\varepsilon_g$ is strongly temperature-dependent, and the temperature-dependence of $\varepsilon_g$ is given in Eq. (4). Expanding Eq. (4) as a power series and truncating the expansion for $T-T_o << \delta$ yields

$$\frac{1}{\varepsilon_g} = \frac{1}{\varepsilon_m} + \frac{(T-T_o)^2}{2\varepsilon_m\delta^2} \qquad \text{for } \delta \gg T-T_o \tag{6}$$

Since $D \cong D_g$, substituting Eq. (6) into Eq. (5) yields the following relationship for the relaxor system having a thin-boundary layer at $T = T_o$[11] :

$$\frac{1}{\varepsilon_c} = \frac{1}{\varepsilon_m} + \frac{1}{R\varepsilon_{gb}} \tag{7}$$

where R is defined as $D_g/D_{gb}$. The thickness of the PbO-rich grain-boundary phase can be calculated using Eq. (7). The peak relative permittivity ($\varepsilon_m$) of 20500 (Fig. 4), $\varepsilon_{gb}$ of 20[25] and $D_g \cong 3\,\mu m$ were used to estimate the thickness of the PbO-rich boundary layer. The calculated thickness of the boundary layer is 0.7 nm. The dielectric analysis thus suggests that a thin intergranular layer on the order of ~1-nm thickness exists in the grain-boundary region. Therefore, the observed increase in the relative permittivity upon annealing can be explained in terms of the elimination of PbO-rich low-permittivity layers.

The observed small difference in the relative dielectric permittivity between the 800°C annealed sample and the 900°C annealed sample (Fig. 4) can now be explained in terms of the PbO-rich intergranular layer. The extent of elimination of the intergranular phase would be at least equal or greater in the specimen annealed at 900°C than in the specimen annealed at 800°C if a process other than the elimination did not occur during annealing. However, as mentioned in the previous section, the content of pyrochlore phase increased to 3% after the an-

nealing at 900°C for 4 h. This suggests that the decomposition of perovskite phase to form pyrochlore phase and PbO-rich phase occurs during the annealing at 900°C, which is caused by thermodynamic instability of PZMN system above a certain critical temperature.[26] Since the decomposition is likely to occur at the grain boundary region rather than at the bulk grain, it is highly probable that the partial decomposition of perovskite phase during the annealing at 900°C is accompanied with the formation of intergranular PbO-rich layer. On the other hand, since the relative content of perovskite phase remains constant (98%) after the annealing at 800°C, a possible decomposition of perovskite phase seems to be dominated by the elimination process at 800°C. Therefore, the intergranular phase is not completely eliminated by the annealing at 900°C, leading to a slight decrease in the relative permittivity compared with that of the PZMN-xPT specimen annealed at 800°C.

The capacitance versus frequency plot exhibits two characteristic regions for the specimen prepared without annealing (Fig. 6). The region (I) is associated with the presence of intergranular layer and corresponds to a small semicircle at a lower frequency region (below 1 kHz) in the complex impedance spectrum.[11] The rapid decrease in the dielectric capacitance (thus dielectric permittivity) with increasing ac frequency for the unannealed specimen in the region (I) indicates the dielectric saturation of space charges in the intergranular layer. The dielectric capacitance in the region (II) is essentially independent of the applied ac frequency. The region (II) corresponds to a conducting mechanism at the perovskite grain.[11] On the other hand, the dielectric capacitance of the 800°C annealed PZMN-0.24PT is essentially independent of the applied ac frequency throughout the whole frequency range (20 Hz ~ 1 MHz), as shown in Fig. 6. This clearly indicates that the observed rapid decrease in the dielectric capacitance for the unannealed specimen in the region (I) is caused by the presence of in-

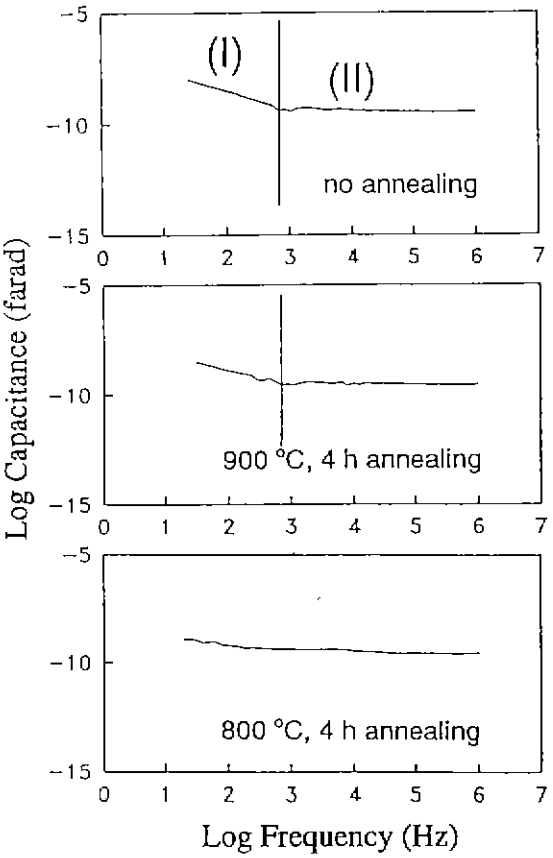


**Fig. 6.** Dielectric capacitance vs ac frequency plot for PZMN-0.24PT specimens prepared with and without thermal annealing after sintering at 1150°C for 1 h.

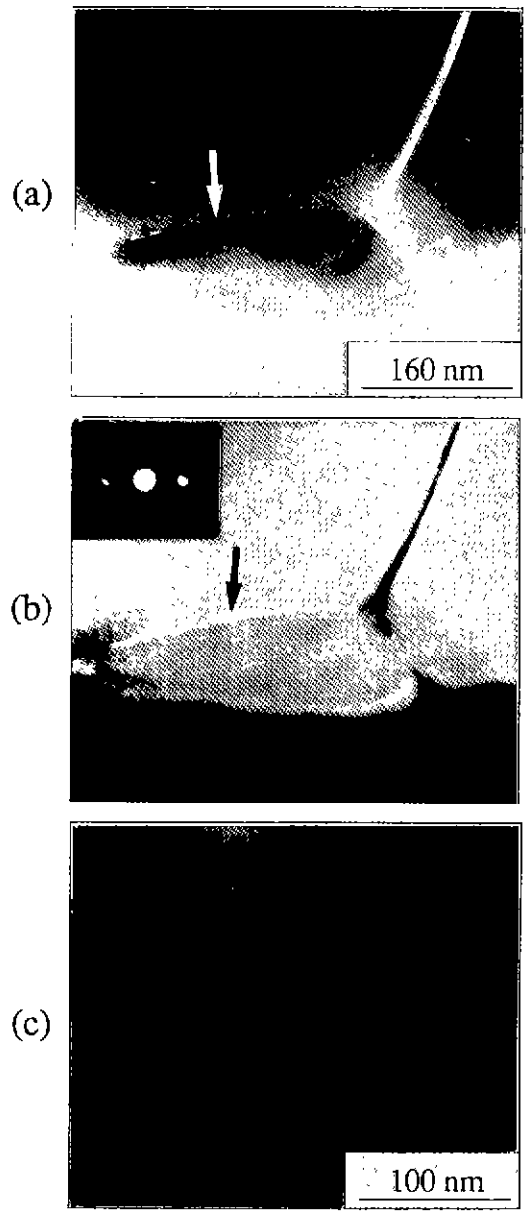


**Fig. 7.** Transmission electron micrographs of PZMN-0.24PT specimens sintered at 1150°C for 1 h : (a) bright-field image of unannealed specimen showing amorphous intergranular layer, (b) dark-field image of unannealed specimen obtained using a halo diffraction pattern, (c) bright-field image of specimen annealed at 800°C for 4 h.

tergranular layer, and this layer can be removed by the annealing at 800°C. The observed decrease in the dielectric capacitance for the 900°C annealed sample in the region (I), as compared to that of the 800°C annealed sample, can be explained in terms of the partial decomposition of perovskite phase to form the intergranular PbO-rich layer at 900°C. Consequently, the intergranular phase is not completely eliminated by the annealing at 900°C, as discussed in the previous paragraph.

A more concrete evidence of the presence of amorphous intergranular layer was obtained by examining the structure of intergranular region microscopically. A typical bright-field image of the unannealed PZMN-0.24PT specimen shows the presence of intergranular layer (Fig. 7 (a)). Since a halo diffraction pattern was observed, the intergranular layer was amorphous. Fig. 7 (b) presents a dark-field image of the unannealed PZMN-0.24PT obtained using a halo pattern, again showing the presence of amorphous intergranular layer. On the contrary, both diffraction study and microscopic examination indicated that the amorphous intergranular layer was absent in the annealed specimen (Fig. 7(c)). Therefore, TEM observations on the boundary regions clearly support the previous conclusion that the observed increase in the relative permittivity upon annealing is directly related with the elimination of amorphous low-permittivity intergranular layers. A high-resolution (HREM) image of the unannealed PZMN-0.24PT indicated that the grain boundary was characterized by a thin layer of about 1 nm thickness.

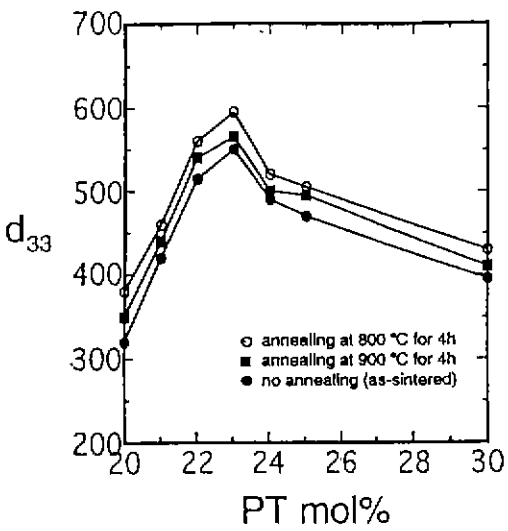


**Fig. 8.** Effect of thermal annealing on piezoelectric constant ($d_{33}$) of PZMN-xPT across morphotropic phase boundary.

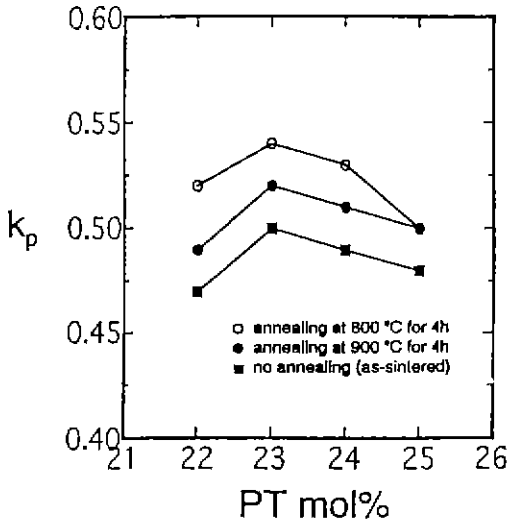


**Fig. 9.** Effect of thermal annealing on electromechanical coupling constant ($k_p$) of PZMN-xPT across morphotropic phase boundary.

### *4. Piezoelectric properties*

The effect of thermal annealing on the piezoelectric constant ($d_{33}$) of PZMN-xPT across the MPB is illustrated in Fig. 8. For the whole range of the composition studied ($0.2 \leq x \leq 0.3$) the piezoelectric constant is increased by the annealing after sintering at 1150°C. This observation again supports the conclusion deduced in the previous section that the change in dielectric/piezoelectric properties upon annealing is directly associated with the elimination of low-permittivity intergranular phase. The difference in $d_{33}$ between the 800°C annealed specimen and the 900°C annealed specimen can be attributed to the difference in the amount of the PbO-rich intergranular phase, as discussed in the previous section. The peak value of $d_{33}$ occurs at x=0.23 which is slightly rhombohedral-rich side of the MPB. This trend is consistent with the previous result of $\varepsilon_r$ for various values of x (Fig. 3).

As shown in Fig. 9, the electromechanical coupling constant ($k_p$) is greatly influenced by annealing. The peak value of $k_p$ also occurs at x=0.23. It was reported that the addition of $SiO_2$ to $Pb(Ni_{1/3}Nb_{2/3})O_3$-$PbTiO_3$-$PbZrO_3$ (PNN-PT-PZ) system enhanced densification but decreased $\varepsilon_r$, $k_t$ (electromechanical coupling constant, thickness mode) and $d_{33}$ significantly.[27] The decrease of $d_{33}$, $k_t$ and $\varepsilon_r$ with increasing content of $SiO_2$ was attributed to the formation of a $SiO_2$-containing intergranular phase derived from the liquid phase above the solubility limit of Si-atoms.[27] Similarly, it was reported that the addition of $V_2O_5$ to $Pb(Zr,Ti)O_3$ (PZT) system reduced sintering temperature significantly, but dielectric/piezoelectric properties were deteriorated by the formation of insulating grain-boundary layers derived from the vanadate liquid phase.[28] Therefore, the observed improvements in the piezoelectric properties of PZMN-xPT upon annealing can also be explained in terms of the elimination of PbO-rich intergranular layers.

## IV. Conclusions

PZMN-xPT polycrystalline ceramics were prepared by

the columbite precursor route, and the dielectric and piezoelectric properties were examined across the rhombohedral/tetragonal MPB ($0.2 \leq x \leq 0.3$). To further improve piezoelectric properties the PZMN-xPT specimens at the MPB composition (x=0.24) were thermally annealed after sintering at 1150°C for 1 h. Both the relative dielectric permittivity and the piezoelectric constant ($d_{33}$)/ electromechanical coupling constant ($k_p$) were increased by the annealing (800~900°C). Based on the dielectric analysis using the series mixing model and the concept of a random Gaussian distribution of the local Curie temperatures, the observed increase in dielectric and piezoelectric constants was interpreted in terms of the elimination of PbO-rich amorphous thin intergranular layers (~1 nm) induced by thermal annealing. The TEM observations on the boundary regions provide a concrete evidence of the presence of thin amorphous grain-boundary layers in the unannealed specimen.

## References


1. J. Kuwata, K. Uchino and S. Nomura, "Phase Transitions in the $Pb(Zn_{1/3}Nb_{2/3})O_3$-$PbTiO_3$ System," *Ferroelectrics*, **37**, 579 -587 (1981).
2. J. Kuwata, K. Uchino and S. Nomura, "Dielectric and Piezoelectric Properties of $0.91Pb(Zn_{1/3}Nb_{2/3})O_3$-$0.09PbTiO_3$ Single Crystals," *Jpn. J. Appl. Phys.*, **22**[9], 1298-1302 (1982).
3. H.M. Jang, S.H. Oh and J.H. Moon, "Thermodynamic Stability and Mechanisms of Formation and Decomposition of Perovskite $Pb(Zn_{1/3}Nb_{2/3})O_3$ Prepared by the PbO Flux Method," *J. Am. Ceram. Soc.*, **75**[1], 82-88 (1992).
4. T.R. Gururaja, A. Safari and A. Halliyal, "Preparation of Perovskite PZN-PT Ceramic Powder near the Morphotropic Phase Boundary," *Am. Ceram. Soc. Bull.*, **65**[12], 1601-1603 (1986).
5. S.L. Swartz and T.R. Shrout, "Fabrication of Perovskite Lead Magnesium Niobate," *Mater. Res. Bull.* **17**, 1245 (1982).
6. J.M. Hayes, T.R. Gururaja, G.L. Geoffroy and L.E. Cross, "Sol-Gel Processing of $0.91Pb(Zn_{1/3}Nb_{2/3})O_3$-$0.09PbTiO_3$ : Stabilization of the Perovskite Phase," *Mater. Lett.* **5**[10], 396-400 (1987).
7. T.R. Shrout and A. Halliyal, "Preparation of Lead-Based Ferroelectric Relaxors for Capacitors," *Am. Ceram. Soc. Bull.*, **66**[4], 704-711 (1987).
8. S. Nomura and K. Uchino, "Recent Applications of PMN-Based Electrostrictors," *Ferroelectrics*, **50**, 197-202 (1983).
9. K. Uchino, "Electrostrictive Actuators : Materials and Applications," *Am. Ceram. Soc. Bull.*, **65**[4], 647 -652 (1986).
10. C.E. Wheeler and B.G. Pazol, "Multilayer Electrodisplacive Actuators," *Am. Ceram. Soc. Bull.*, **70**[1], 117-119 (1991).
11. H.M. Jang, K.-M. Lee, and M.-H. Lee, "Stabilization of Perovskite Phase and Dielectric Properties of Pb $(Zn,Mg)_{1/3}Nb_{2/3}O_3$-$PbTiO_3$ Ceramics Prepared by Excess Constituent Oxides," *J. Mater. Res.* **9**, 2634-2644 (1994).
12. L. Hanh, K. Uchino, and S. Nomura, "On the Phenomenon of Morphotropic Tetragonal-Rhombohedral Phase Boundary in the Ferroelectric Ceramics," *Jpn. J. Appl. Phys.*, **17**, 637 (1978).
13. S.M. Landin and W.A. Schulze, "Rapid Sintering of Stoichiometric Zinc-Modified Lead Magnesium Niobate," *J. Am. Ceram. Soc.*, **73**[4], 913-918 (1990).
14. Y. Yokomizo, T. Takahashi and S. Nomura, "Ferroelectric Properties of $Pb(Zn_{1/3}Nb_{2/3})O_3$," *J. Phys. Soc. Jpn.*, **28**[5], 1278-1284 (1970).
15. J. Kuwata, K. Uchino, and S. Nomura, "Diffuse Phase Transitions in Lead Zinc Niobate," *Ferroelectrics*, **22**, 863-867 (1979).
16. S.W. Choi, T.R. Shrout, S.J. Jang and A.S. Bhalla, "Dielectric and Pyroelectric Properties in the $Pb(Mg_{1/3}Nb_{2/3})O_3$-$PbTiO_3$ System," *Ferroelectrics*, **100**, 29-38 (1989).
17. L.L. Hench and J.K. West, Principles of Electronic Ceramics (John Wiley & Sons, 1990), Chap., **6**.
18. G.M. Smolenskii, "Physical Phenomena in Ferroelectrics with Diffused Phase Transition," Proc. Int. Meet. Ferroelectr., 2nd, 1969, 26-36 (1970).
19. B.N. Rolov, "Effect of Composition Fluctuations on Unsharp Phase Transitions," *Sov. Phys.-Solid State* (Engl. Transl.), **6**, 1676-1678 (1965).
20. S.M. Pilgrim, A.E. Sutherland, and S.R. Winzer, "Diffuseness as a Useful Parameter for Relaxor Ceramics," *J. Am. Ceram. Soc.*, **73**[10], 3122-3125 (1990).
21. M.P. Harmer, J. Chen, P. Peng, H.M. Chan and D.M. Smyth, "Control of Microchemical Ordering in Relaxor *Ferroelectrics*, and Related Compounds," *Ferroelectrics*, **97**, 263-274 (1989).
22. J. Chen, H.M. Chan and M.P. Harmer, "Ordering Structure and Dielectric Properties of Undoped and La/Na-doped $Pb(Mg_{1/3}Nb_{2/3})O_3$," *J. Am. Ceram. Soc.*, **72**[4], 593-598 (1989).
23. H.-C. Wang and W.A. Schulze, "The Role of Excess Magnesium Oxide or Lead Oxide in Determining the Microstructure and Properties of Lead Magnesium Niobate," *J. Am. Ceram. Soc.*, **73**[4], 825-832 (1990).
24. C.A. Randall, A.D. Hilton, D.J. Barber and T.R. Shrout, "Extrinsic Contributions to the Grain Size Dependence of Relaxor Ferroelectric $Pb(Mg_{1/3}Nb_{2/3})O_3$:$PbTiO_3$ Ceramics," *J. Mater. Res.*, **8**, 880-884 (1993).
25. P. Papet. J.P. Dougherty and T.R. Shrout, "Particle and Grain Size Effects on the Dielectric Behavior of the Relaxor Ferroelectric $Pb(Mg_{1/3}Nb_{2/3})O_3$," *J. Mater. Res.*, **5**, 2902 - 2909 (1990).
26. H.M. Jang, S.R. Cho and K.-M. Lee, "Mechanism of Formation of Perovskite Phase and Dielectric Properties of $Pb(Zn,Mg)_{1/3}Nb_{2/3}O_3$ Ceramics Prepared by Columbite Precursor Routes," *J. Am. Ceram. Soc.*, **78**[2], 297-304 (1995).
27. J.H. Moon and H.M. Jang, "Densification Behavior and Piezoelectric Properties of $MnO_2$, $SiO_2$-doped $Pb(Ni_{1/3}Nb_{2/3})O_3$-$PbTiO_3$-$PbZrO_3$ Ceramics," *J. Mater. Res.*, **8**, 3184-3191 (1993).
28. D.E. Wittmer and R.C. Buchanan, "Low-Temperature Densification of Lead Zirconate-Titanate with Vanadium Pentoxide Additive," *J. Am. Ceram. Soc.*, **64**[8], 485-490 (1981).